Journal of Electrochemistry

Volume 27 | Issue 6

2021-12-28

Nitrogen-Sulfur Co-Doped Porous Carbon Preparation and Its Application in Lithium-Sulfur Batteries

Zhao Gui-Xiang

Hafiz Zaki Ahmed Wail

Zhu Fu-Liang

1. School of Materials Science and Engineering, Lanzhou University of Technology, Lanzhou 730050, Gansu, China;2. State Key Laboratory of Advanced Processing and Recycling of Nonferrous Metals,Lanzhou 730050, Gansu, China,, chzfl@126.com

In recent years, lithium-sulfur (Li-S) batteries have been considered as a promising candidate for the next generation of energy storage system due to their ultrahigh theoretical capacity (1675 $mAh \cdot g^{-1}$) and energy density (2600 $Wh \cdot kg^{-1}$). However, the practical application of Li-S batteries is severely limited by their insulating nature of sulfur, the shuttle effect of polysulfides (LiPSs), and volume expansion during charging and discharging. To overcome those disadvantages, one of the commonly methods is to infiltrate sulfur into porous conductive carbon framework, such as porous carbon, hollow carbon spheres, graphene, carbon nanotubes and some composites of the above structures to achieve the purpose of physically limiting the shuttle effect of polysulfides, thereby improving the performance of Li-S batteries. However, due to the nonpolarity of traditional carbon materials, the interaction with polar polysulfides is very weak, which cannot effectively inhibit the shuttle effect of polysulfides. Previous studies have shown that introducing heteroatom (N, S, P, B, etc.) doping into carbon matrix is a feasible method to adjust the nonpolarity of carbon materials. It is reported that the introduction of N atoms is conducive to improving the electrochemical activity. The Li-N bond formed by the interaction between N and Li^+ can anchor polysulfides, effectively inhibit the dissolution of polysulfides and improve the utilization rate of sulfur. The introduction of nitrogen and sulfur heteroatoms can increase polar sites and active centers, thus, enhancing the adsorption capacity of carbon materials for polysulfides and capturing polysulfides. Therefore, ionic liquids are selected as nitrogen and sulfur sources to improve the polarity of carbon materials. In this paper, nitrogen and sulfur co-doped porous carbon (NSPC) was synthesized by using glucose as carbon source, KCl and $ZnCl_2$ as templates, KOH as activator and ionic liquid as heteroatom source. XPS and adsorption experiments show that nitrogen and sulfur heteroatoms had been successfully introduced into NSPC, which improved the adsorption capacity of carbon materials for polysulfides, effectively alleviated the shuttle effect of polysulfides. The higher specific surface area (1290.67 $m^2 \cdot g^{-1}$) could help to improve the sulfur loading. After loading 70.1wt.% sulfur into NSPC (S@NSPC) and tested as a cathode material of Li-S battery, the initial discharge capacity was 1229.2 $mAh \cdot g^{-1}$ at 167.5 $mA \cdot g^{-1}$, higher than the 861.6 $mAh \cdot g^{-1}$ of S@PC, and the capacity remained at 328.1 $mAh \cdot g^{-1}$ after 500 cycles. When the current density returned to 167.5 $mA \cdot g^{-1}$, the reversible capacity almost went back to its initial value, which was 80% of its initial value. The good performance was mainly ascribed to both the porous structure and N, S co-dopants, which provided physical blocks and chemical affinity, respectively, for the efficient immobilization of intermediate lithium polysulfides. The results would provide an effective example in the surface chemistry and sulfur host materials design for high performance Li-S batteries.

Available at: https://jelectrochem.xmu.edu.cn/journal/vol27/iss6/8

第 27 卷 第 6 期
2021 年 12 月

电化学
JOURNAL OF ELECTROCHEMISTRY

Vol. 27 No. 6
Dec. 2021

【Article】 **DOI**: 10.13208/j.electrochem.201210 **Http**://electrochem.xmu.edu.cn

氮硫共掺杂多孔碳材料的制备及其在锂硫电池中的应用

赵桂香[1], Wail Hafiz Zaki Ahmed[1], 朱福良[1,2*]

(1. 兰州理工大学材料科学与工程学院, 甘肃 兰州 730050;
2. 有色金属先进加工与再利用国家重点实验室, 甘肃 兰州 730050)

摘要: 锂硫电池因其较高的理论容量和对环境友好等优势被视为极具发展潜力的储能装置, 但是多硫化物的穿梭效应极大地限制了锂硫电池的实际应用。本文以葡萄糖为碳源, 离子液体为氮源和硫源, KCl和$ZnCl_2$为模板剂, KOH为活化剂, 通过热解工艺合成了氮硫共掺杂多孔碳(NSPC)。XPS和极性吸附实验表明N、S杂原子成功引入并且提高了碳材料对多硫化物的吸附能力, 有效缓解多硫化物的穿梭效应, 而较高的比表面积(1290.67 $m^2 \cdot g^{-1}$)有助于提高硫负载量。负载70.1wt.%的硫后(S@NSPC)作为锂硫电池的正极材料表现出了良好的电化学性能。在167.5 $mA \cdot g^{-1}$的电流密度下S@NSPC的首次放电容量为1229.2 $mAh \cdot g^{-1}$, 远高于S@PC的861.6 $mAh \cdot g^{-1}$, 且S@NSPC循环500圈后容量为328.1 $mAh \cdot g^{-1}$。当电流密度从3350 $mA \cdot g^{-1}$恢复至167.5 $mA \cdot g^{-1}$时, 可逆容量达到首圈放电比容量的80%, 几乎恢复至其初始值。

关键词: 锂硫电池; 多孔碳; N、S共掺杂

1 引 言

近年来, 便携式电子产品、电动汽车等领域的迅速发展, 使得对高效储能技术的需求日益迫切[1], 而目前被广泛使用的锂离子电池已接近其理论比能量的上限, 无法完全满足储能需求[2]。在众多的储能技术中, 锂硫(Li-S)电池因硫储量丰富, 环境友好且具有较高的能量密度(2600 $wh \cdot kg^{-1}$)和较高的理论容量(1675 $mAh \cdot g^{-1}$)等优点, 引起了研究者们的广泛关注[3-8]。但是 Li-S 电池在实际应用中仍然面临着许多挑战: (1)硫(在 25 ℃ 下为 5×10^{-30} $S \cdot cm^{-1}$)及其最终产物多硫化锂(Li_2S_2/Li_2S)的低导电率, 导致硫的利用率较低; (2)硫(2.03 $g \cdot cm^{-3}$)和硫化锂(1.66 $g \cdot cm^{-3}$)的密度差异较大, 在充放电过程中伴随着很大的体积膨胀(80%), 在多次充放电过程后会破坏电极结构, 导致电极材料粉化而引起容量的下降; (3)充放电过程中多硫化锂易溶于电解液, 在正负极之间穿梭, 导致活性物质硫的不可逆损失[9-15]。其中, 多硫化锂的穿梭效应是影响锂硫电池性能的主要因素。

为了解决上述问题, 研究者们致力于设计各种结构的材料(多孔碳[16, 17]、石墨烯[18, 19]、CNT[20]和金属化合物[21-23]等)作为硫的载体, 其中碳材料因其良好的导电性、优异的机械延展性和化学稳定性等优点在很多领域被广泛使用, 且多孔碳具有可调的比表面积和独特的孔道结构, 有助于阻隔多硫化锂并减少其在电解液中的溶解, 从而提高硫的利用率。但非极性的碳材料与极性的多硫化锂之间相互作用力较弱, 从而无法有效的抑制穿梭效应[24], 而杂原子(N、B、S、P 等)的掺杂是提高碳材料极性行之有效的方法[25-29]。因此, 设计一种

引用格式: Zhao G X, Zaki Ahmed W H, Zhu F L. Nitrogen-sulfur co-doped porous carbon preparation and its application in lithium-sulfur batteries. *J. Electrochem.*, 2021, 27(6): 614-623.

收稿日期: 2020-12-10, 修订日期: 2021-02-02. *通讯作者: Tel: (86-931)2973942, E-mail:chzfl@126.com
国家自然科学基金项目(No. 52064035)和甘肃省自然科学基金(No. 20JR10RA166)资助

具有杂原子掺杂和高比表面积的碳材料来抑制多硫化锂的穿梭效应是极其重要的。

本文采用葡萄糖作为碳源，离子液体作为杂原子源,KOH 作为活化剂，经过简单的热解处理，成功制备出了氮硫共掺杂多孔碳，该材料具有较高的比表面积(1290.67 $m^2 \cdot g^{-1}$),这是高载硫的必要条件。同时,N、S 杂原子的掺杂增强了碳材料的极性,可以对极性多硫化物进行有效吸附,进而在一定程度上抑制穿梭效应。当载硫后将其作为 Li-S 电池正极材料时表现出了良好的循环稳定性和倍率性能。

2 实　验

2.1 试剂与仪器

葡萄糖、氯化锌、氯化钾、氢氧化钾、升华硫、聚偏氟乙烯(PVDF)和 N- 甲基吡咯烷酮(NMP)均为分析纯，购自上海阿拉丁生化科技股份有限公司;浓盐酸(分析纯)购自国药集团化学试剂有限公司;电解液(电池级)购自厦门科路德科技有限公司;乙炔黑(电池级)购自科晶智达科技有限公司。

采用 X 射线衍射(XRD)(Bruker D8 Advance,Cu K_α 辐射)在 10° ~ 60°的 2θ 范围内表征该复合材料的结构。采用扫描电子显微镜(SEM,JEOL-6701F)观察复合物的形貌。采用 Brunauer-Emmelt-Teller(BET)来分析计算复合材料的比表面积和孔径分布。

2.2 材料的制备

在材料的合成中,模板剂 KCl 与 $ZnCl_2$ 的质量比为 5:7,模板剂与葡萄糖的质量比为 1:6,葡萄糖与活化剂 KOH 的质量比为 1:3,进行研磨,再加入 0.5 g 的 1-乙基-3-甲基咪唑硫酸氢盐和适量的乙醇研磨直至均匀。接着将其转移至坩埚中,在氩气气氛保护的管式炉中升温至 800 ℃,升温速率为 3 ℃·min^{-1},保温 1 小时后自然冷却。最后,将制备的碳材料研磨，用盐酸和去离子水各洗涤 10 次,并在 80 ℃ 下保温 12 小时获得氮硫共掺杂多孔碳材料(NSPC)。多孔碳(PC)的制备过程与 NSPC 过程一致,只是没有添加杂原子源。

将上述合成的氮硫共掺杂多孔碳升华硫按 1:3 的质量比混合,研磨半小时后转移至聚四氟乙烯高压反应釜中,于 155 ℃ 下保温 12 小时,将得到的产物记为 S@NSPC。合成多孔碳硫复合物的过程与上述一致,记为 S@PC。

2.3 电池的组装

将上述合成的碳硫复合物、乙炔黑、粘结剂按质量比为 7:2:1 与溶剂 NMP 混合均匀，涂覆在铝箔上,在烘箱中于 80 ℃ 干燥 12 小时,将其切成直径为 12 mm 的圆片作为工作电极，锂片作为对电极，型号 Celgard 2400 为隔膜，含有浓度为 0.2 mol·L^{-1} $LiNO_3$ 的 1,3 二氧戊环 /1,2-二甲氧基乙烷(DOL/DME)(1:1,V/V)的 1 mol·L^{-1} 的双(三氟甲烷)磺酰亚胺锂(LiTFSI)为电解液,在充满氩气的手套箱中组装成 CR2032 型扣式电池，静置 12 h 后进行电化学性能测试。在电化学工作站上进行循环伏安法(CV)测试,扫描速率为 0.1 mV·s^{-1},电压范围为 1.7 ~ 2.8 V,电化阻抗(EIS)的测量频率范围为 0.01 ~ 10^5 Hz。

3 结果与分析

NSPC 的 SEM 如图 1(A)所示。从图中可以看

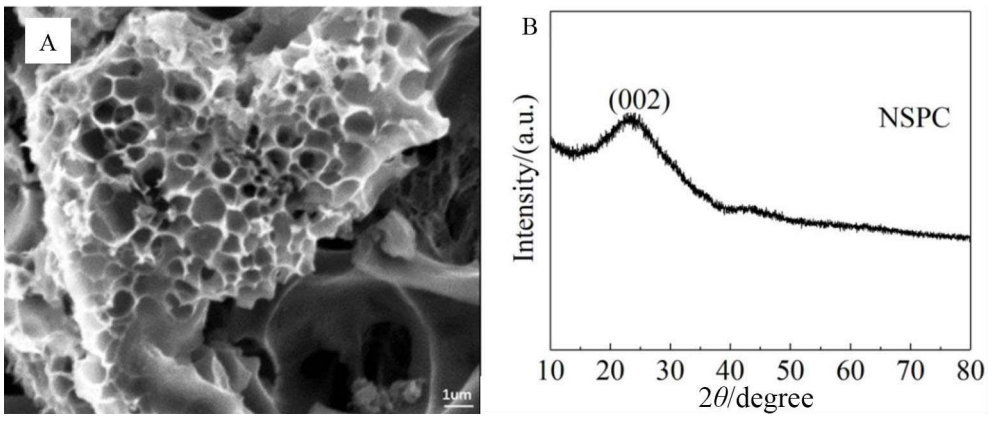

图1 (A) NSPC的SEM照片和(B)XRD图谱

Figure 1 (A) SEM image and (B) XRD pattern of NSPC

出碳材料表面分布着均匀的孔，这是由于 KOH 在高温下与碳反应产生大量的挥发性气体如 CO_2，而 CO_2 作为成孔剂在碳材料中形成丰富的孔[30]。图 1(B)为 NSPC 的 XRD 图谱，在 22° 附近存在明显的宽峰，对应为无定型碳(002)面的衍射峰[30]。

S@NSPC 的 SEM 如图 2(A)所示，从图中可以发现碳材料表面沉积着均匀的硫，且硫之间存在间隙，有助于电解液的渗透。图 2(B)所示为 S@NSPC 的 XRD 图谱，在 2θ 约为 23.1、26、27.8 和 32° 处出现了明显的特征峰，对应于 S 的(222)、(026)、(040)、(044)面，这与 S 的标准 PDF 卡片相一致，说明 S 成功负载到碳材料中[31]。在图谱中并没有出现 KCl、$ZnCl_2$ 和 KOH 的衍射峰，表明盐模板和活化剂已被去除干净。

采用 XPS 分析了 NSPC 的元素组成，结果表明样品中存在 C、N、O 和 S 元素，且 N、S 的含量分别为 6.51%和 0.37%。在图 3(B)的 C 1s 光谱中，位于 284.7、285.5、286.8 和 290.2 eV 处的四个峰分别归因于 C-C/C =C、C-S、C-O 和 O-C=O 键[25]。图 3(C)的 N 1s 光谱中，位于 398.6、400.1、401.2 和 405.2 eV 处的四个峰分别归因于吡啶氮、吡咯氮、石墨氮和氧化氮[20]。已有研究表明，引入吡啶氮和吡咯氮可以通过提供更多的活性位点来改善电池的电化学性能[25]，氮掺杂使碳材料具有更多的极性位点，可以增强多孔碳材料对多硫化物的吸附[20]。图 3(D)的 S 2p 光谱显示了在 165.2、164.0 和 168.9 eV 处的三个峰，分别对应 S $2p^{1/2}$、S $2p^{3/2}$ 和 SO_x，而 SO_x 可能是硫在空气中被氧化引起的[27, 32]。N、S 掺杂可以改变碳材料表面的电子结构并产生更多的活性位点，从而增强碳材料的表面极性[26]，达到抑制多硫化锂穿梭的目的。

NSPC 的 N_2 吸附-脱附等温线和孔径分布曲线如图 4(A、B)所示。从图 4(A)中可以看出曲线属于 I 型和 IV 型曲线，说明 NSPC 中存在微孔和介孔，并且在较低的相对压力下($P/P_0 < 0.1$)具有高的 N_2 吸附量，表明 NSPC 存在微孔[33]，而滞后环的存在表明 NSPC 中存在介孔[25]。根据 Barrett-Joyner-Halenda(BJH)方法(图 4(B))得出的孔径分布曲线进一步证明 NSPC 存在 < 2 nm 的微孔、大量 2 ~ 10 nm 的介孔和少量 > 50 nm 的大孔，显然 NSPC 是由微孔、介孔和大孔共同组成。NSPC 的比表面积、孔径和孔容分别为 1290.67 $m^2 \cdot g^{-1}$、4.76 nm 和 1.53 $cm^3 \cdot g^{-1}$，已有实验表明较高的比表面积和孔隙体积为硫的负载提供更大的空间，并为多硫化物提供更多的活性位置，从而减轻穿梭效应[25]。

为了进一步研究硫的分布，碳硫复合物(S@NSPC)的氮气吸附-脱附等温曲线如图 5 所示。从图 5(A)中可以发现曲线属于 IV 型曲线，存在滞后环，表明 S@NSPC 中存在介孔，微孔几乎消失。并且从该曲线可以看出相比于未负载硫时的曲线(图 4(A))，S@NSPC 在低压区具有较小的 N_2 吸附量，比表面积也急剧下降，从 1290.67 $m^2 \cdot g^{-1}$ 下降至 60.48 $m^2 \cdot g^{-1}$。从图 5(B)孔径分布图中可以看出在 S@NSPC 中的微孔在减少，并且孔容从 1.53 $cm^3 \cdot g^{-1}$ 下降至 0.198 $cm^3 \cdot g^{-1}$。这个结果说明 S@NSPC 的孔被硫占据[34, 35]。

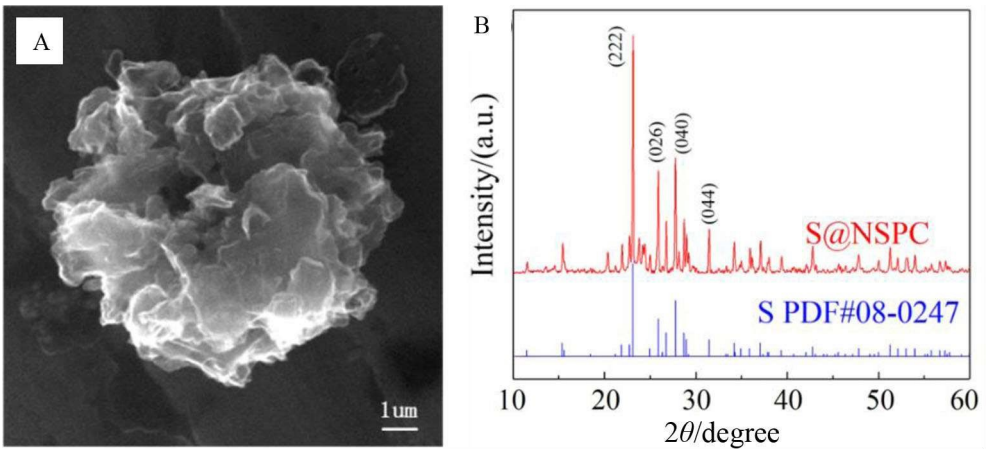

图2 (A)S@NSPC的SEM图像；(B) S@NSPC的XRD图谱 (网络版彩图)

Figure 2 (A) SEM image and (B) XRD pattern (compared with the standard lines of S) of S@NSPC (color on line)

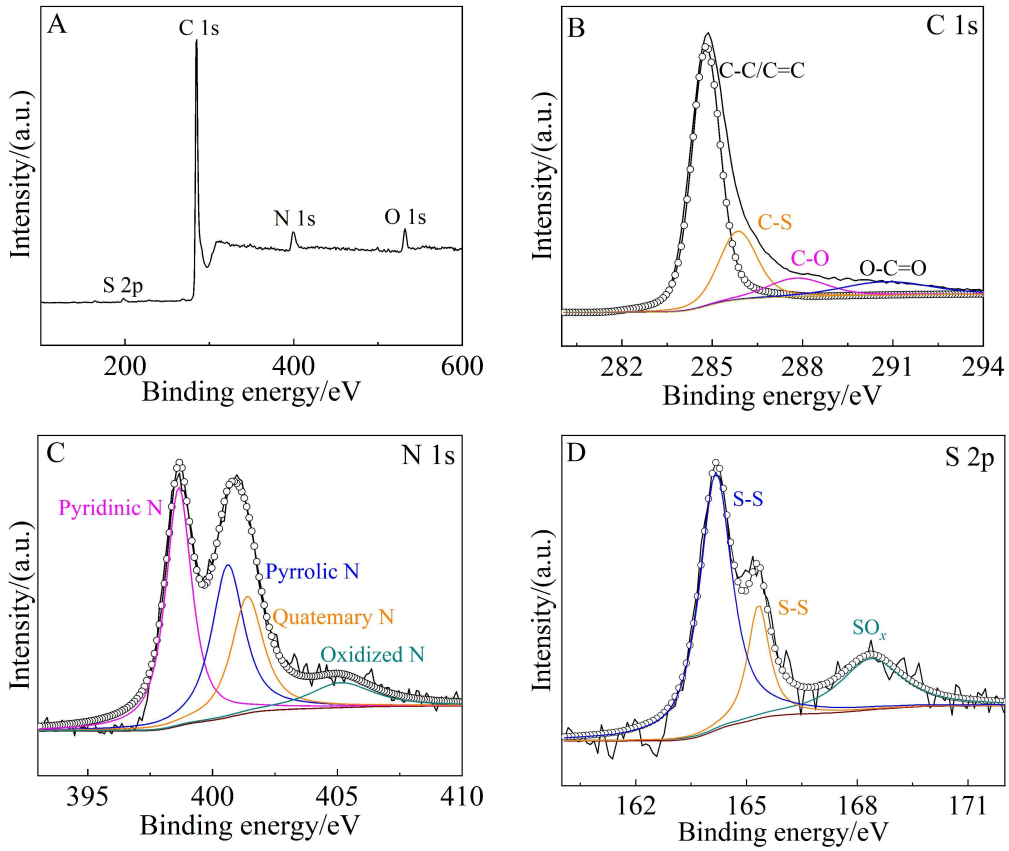

图3 NSPC的XPS图谱: (A) C 1s、N 1s和S 2p的总谱; (B) C 1s;(C) N 1s;和(D) S 2p (网络版彩图)

Figure 3 XPS data of NSPC (A) Elemental survey; (B) C 1s; (C) N 1s; (D) S 2p (color on line)

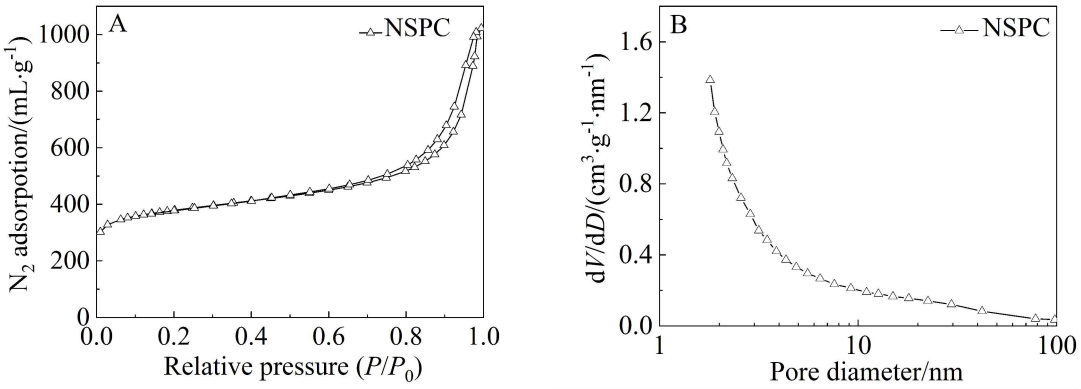

图4 (A、B)NSPC在低温下的氮气吸附-脱附等温曲线和孔径分布图

Figure 4 (A、B) Nitrogen adsorption-desorption isotherm and pore size distribution diagram of NSPC at low temperature

较大的比表面积和多孔结构在提高硫含量和抑制多硫化物的穿梭效应方面起着重要的作用。据报道，较大的比表面积可以为硫的负载提供更多的空间。多孔结构有利于捕获多硫化物,微孔由于较小的孔径尺寸以及较强的毛细作用,可以起到有效的固硫作用[35],而当孔径过大时,无法起到有效的固硫作用，从而无法抑制多硫化物的穿梭效应。

为了直观地反应N、S共掺杂多孔碳材料(NSPC)极性吸附能力,我们进行了多硫化物溶液的吸附实验。将等量的NSPC和对比样乙炔黑分别放入装有多硫化锂溶液的瓶中，然后对瓶中溶液

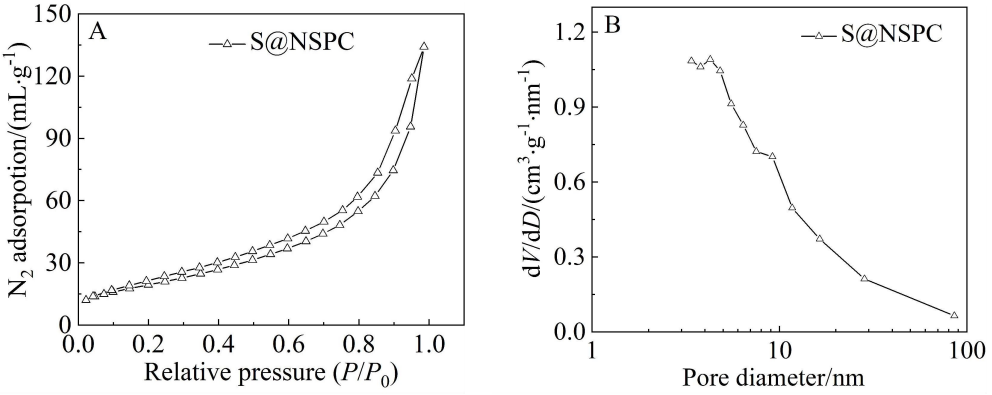

图5 S@NSPC在低温下的氮气吸附-脱附等温曲线(A)和孔径分布图(B)

Figure 5 Nitrogen adsorption-desorption isotherm (A) and pore size distribution diagram (B) of S@NSPC at low temperature

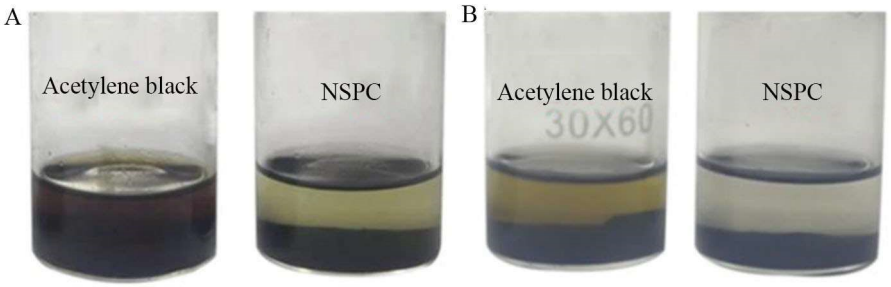

图6 NSPC和对比样的吸附测试:(A) 0.5 h;(B) 12 h (网络版彩图)

Figure 6 Adsorption tests of NSPC and contrast sample: (A) 0.5 h; (B) 12 h (color on line)

的颜色变化进行观察,结果如图6所示。观察发现经过0.5小时后加入了NSPC的溶液颜色变化比乙炔黑的明显，而12小时后两者颜色均在一定程度上变浅,但加入了NSPC的溶液颜色变化更加明显并趋于透明,这个结果说明NSPC具有较强的多硫化物吸附能力。

通过在惰性气氛,升温速率为10 ℃·min^{-1}的条件下进行热重测试可以得知S@NSPC中硫的含量。从图7的曲线中可以看出在150 ℃附近开始出现失重,在150 ℃ ~ 280 ℃之间快速失重,这可能是由于负载到表面或是较大孔中的硫被蒸发,在此阶段硫的失重量约为53.6wt.%，而在280 ℃ ~ 400 ℃之间的失重可能归因于介孔和微孔中硫的蒸发,由于微孔的毛细作用使得微孔中的硫需在高温下才能脱离碳基体[36],在此阶段的失重量约为16.5wt.%,根据计算显示S@NSPC中的总失重量约为70.1wt.%,表明S@NSPC中的硫含量约为70.1wt.%。

采用循环伏安法(CV)来研究S@NSPC的电化学过程(电压范围1.7 ~ 2.8 V,扫描速率0.1 mV·s^{-1}),

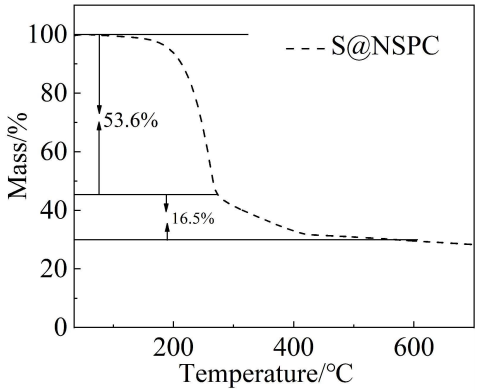

图7 S@NSPC的热重曲线

Figure 7 TGA curve of S@NSPC

如图8(A)所示。在负向扫描中,观察到S@NSPC位于约2.30 V和2.0 V的两个尖锐的还原峰,分别对应于S_8还原为高阶多硫化锂(Li_2S_n, $4 < n < 8$)和低阶多硫化锂(Li_2S_2/Li_2S)的过程[37, 38]。在正向扫描中,观察到在2.38 V和2.4 V处存在两个氧化峰，分别对应于低阶的多硫化锂被氧化成高阶的多硫化锂

和S_8[39, 40]的过程。但从第2圈开始S@NSPC表现出更尖锐和重叠的氧化还原峰,表明S@NSPC具有优异的电化学可逆性。图8(B)为S@NSPC在电压范围为1.7～2.8 V,电流密度为167.5 mA·g^{-1}下的恒流充放电曲线。首圈充放电比容量为1229.2/1070.3 mAh·g^{-1},而循环3圈后容量为907.3/869.3 mAh·g^{-1},说明S@NSPC具有良好的循环稳定性,N、S共掺杂增强了碳材料对多硫化物的捕获。

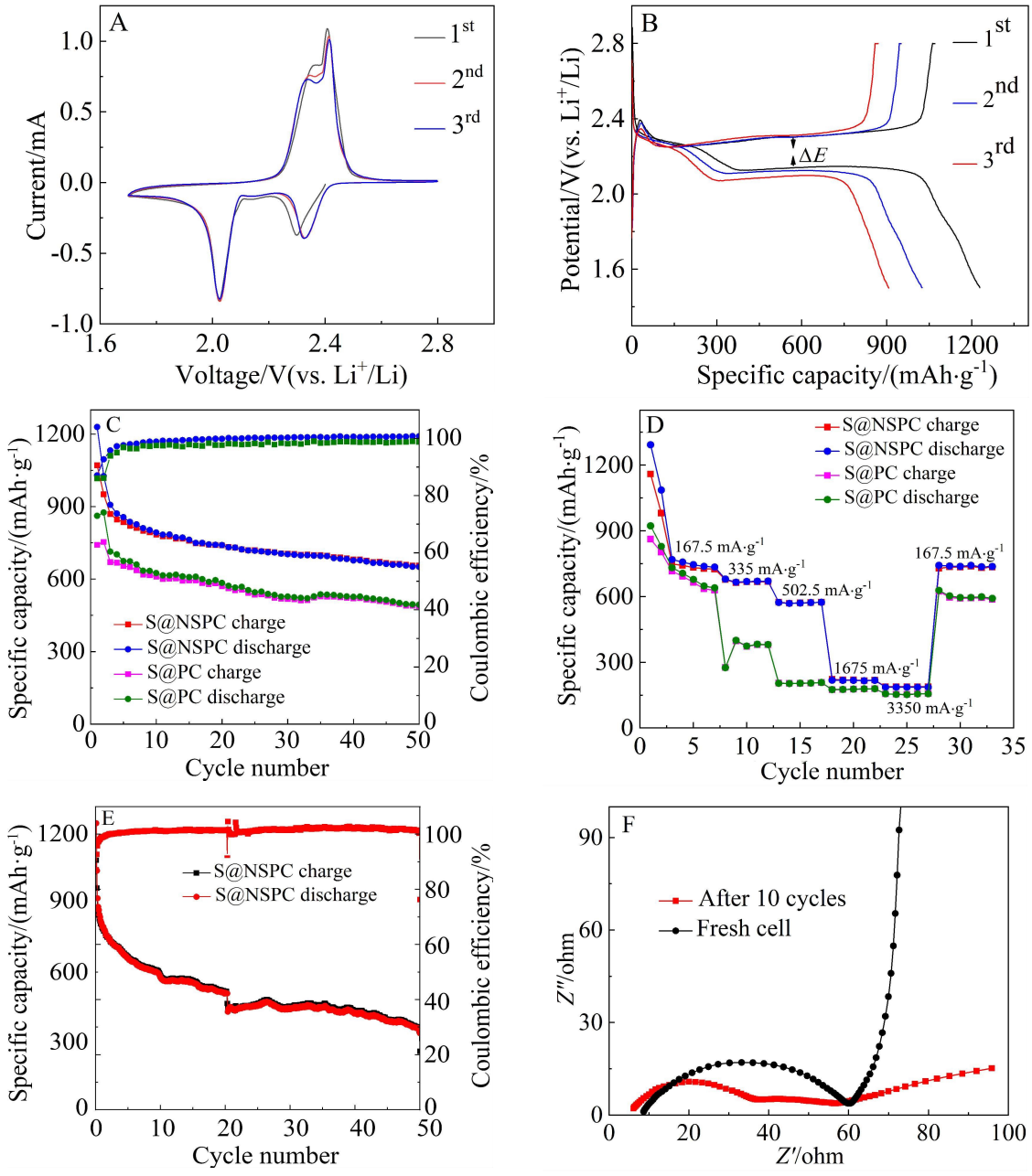

图8 (A) S@NSPC在扫速为0.1 mV·s^{-1}时的循环伏安曲线,(B) S@NSPC的恒电流充放电曲线,(C) S@NSPC和S@PC的循环性能曲线,(D) S@NSPC和S@PC在不同电流密度下的倍率性能曲线,(E) S@NSPC在电流密度为167.5 mA·g^{-1}下的长循环容量曲线,(F) S@NSPC 循环前和循环10圈后的交流阻抗谱 (网络版彩图)

Figure 8 (A) CV curves of S@NSPC at a sweep rate of 0.1 mV·s^{-1}, (B) Galvanostatic discharge/charge curves of S@NSPC at 167.5 mA·g^{-1}, (C) Cycling performance curves of S@NSPC and S@PC electrodes at a current density of 167.5 mA·g^{-1}, (D) Rate performance curves of S@NSPC and S@PC, (E) Long cycle performance of S@NSPC at a current density of 167.5 mA·g^{-1}, (F) Nyquist plots of S@NSPC before cycling and after 10 cycles (color on line)

图8(C)是S@NSPC和S@PC在电流密度为167.5 mA·g^{-1}下的循环性能曲线。从图可以看出，S@NSPC和S@PC在167.5 mA·g^{-1}电流密度下首圈放电比容量分别为1229.2 mAh·g^{-1}和861.6 mAh·g^{-1}。在循环50圈后S@NSPC的放电容量仍然保持在650.9 mAh·g^{-1}，而S@PC的容量降至493.8 mAh·g^{-1}。相比于S@PC，S@NSPC具有高可逆容量，可能原因是氮硫杂原子的掺杂增加了碳材料对可溶性多硫化物的捕获能力，S@NSPC经过500圈的循环后可逆容量能保持在328.1 mAh·g^{-1}，如图8(E)所示。已有研究表明，N、S杂原子的掺杂不仅能对多硫化锂进行强吸附而且还能显著增强碳材料的导电率，从而提高硫的利用率。

图8(D)为S@NSPC和S@PC在不同电流密度下的倍率性能曲线。其中，S@NSPC在167.5、335、837.5、1675和3350 mA·g^{-1}的电流密度下可逆容量分别为927.0、679.7、573.2、218.0和186.4 mAh·g^{-1}。当电流密度为3350 mA·g^{-1}时S@NSPC的可逆容量能保持在186.4 mAh·g^{-1}。从图中可以发现，在各电流密度下S@NSPC的可逆容量均高于S@PC，在335 mA·g^{-1}的电流密度下S@PC的容量已经开始骤降，而S@NSPC则下降缓慢，这表明S@NSPC在经过大的电流冲击后容量依然可以恢复。为了验证充放电容量的可逆性，将电流密度从3350 mA·g^{-1}恢复至167.5 mA·g^{-1}时，S@NSPC的放电容量几乎恢复了其初始值，是首圈放电比容量的80%，这表明其具有良好的倍率性能。

图8(F)为S@NSPC循环前和循环10圈后在0.01 ~ 100 kHz频率范围内的阻抗图。在循环前，阻抗图由高频区的一个半圆和低频区的一条斜线组成，这分别归因于电荷转移电阻和离子扩散过程。而循环10圈后出现了高频区的一个半圆和中频区的一个半圆，分别对应于界面电阻(R_{SEI})和电荷转移电阻(R_{ct})[22, 41]，从图中可以看出循环后的R_{ct}值小于循环前的，这是由于电池刚开始循环时，硫分布不均匀导致的，而在随后的循环中硫被活化再分散，从而S@NSPC具有较小的阻抗。

4 结 论

本文选用葡萄糖为碳源、离子液体为杂原子源，KOH为活化剂，制备了N、S共掺杂多孔碳材料，该材料具有丰富的孔隙度，较大的比表面积(1290.67 m^2·g^{-1})以及丰富的杂原子掺杂。S@NSPC能够通过多孔结构的物理连接和N、S杂原子的化学吸附有效地捕获可溶性多硫化锂，从而有效改善循环性能和倍率性能。S@NSPC电极在167.5 mA·g^{-1}电流下的初始放电容量为1229.2 mAh·g^{-1}，高于S@PC电极的861.6 mAh·g^{-1}，在循环500次后，S@NSPC仍可保持328.1 mAh·g^{-1}的高容量。当从高电流密度(3350 mA·g^{-1})恢复至低电流密度(167.5 mA·g^{-1})时可逆容量几乎恢复至其初始值，是首圈放电比容量的80%。

参考文献(References):

[1] Rehman S, Gu X X, Khan K, Mahmood N, Yang W L, Huang X X, Guo S, Hou Y L. 3D vertically aligned and interconnected porous carbon nanosheets as sulfur immobilizers for high performance lithium-sulfur batteries [J]. Adv. Energy Mater., 2016, 6(12): 1502518.

[2] Yang W W, Xiao J W, Ma Y, Cui S Q, Zhang P, Zhai P B, Meng L J, Wang X G, Wei Y, Du Z G, Li B X, Sun Z B, Yang S B, Zhang Q F, Gong Y J. Tin intercalated ultrathin MoO_3 nanoribbons for advanced lithium-sulfur batteries [J]. Adv. Energy Mater., 2019, 9(7): 1803137.

[3] Yu M P, Ma J S, Xie M, Song H Q, Tian F Y, Xu S S, Zhou Y, Li B, Wu D, Qiu H, Wang R M. Freestanding and sandwich-structured electrode material with high areal mass loading for long-life lithium-sulfur batteries[J]. Adv. Energy Mater., 2017, 7(11): 1602347.

[4] Chen S X, Luo J H, Li N Y, Han X X, Wang J, Deng Q, Zeng Z L, Deng S G. Multifunctional LDH/Co_9S_8 heterostructure nanocages as high-performance lithium-sulfur battery cathodes with ultralong lifespan[J]. Energy Stor. Mater., 2020, 30: 187-195.

[5] Guo D Y, Wei H F, Chen X A, Liu M L, Ding F, Yang Z, Yang Y, Wang S, Yang K Q, Huang S M. 3D hierarchical nitrogen-doped carbon nanoflower derived from chitosan for efficient electrocatalytic oxygen reduction and high performance lithium-sulfur batteries[J]. J. Mater. Chem. A, 2017, 5(34): 18193-18206

[6] Cheng X B, Huang J Q, Zhang Q, Peng H J, Zhao M Q, Wei F. Aligned carbon nanotube/sulfur composite cathodes with high sulfur content for lithium-sulfur batteries [J]. Nano Energy, 2014, 4: 65-72.

[7] Chen M F, Jiang S X, Huang C, Wang X Y, Cai S Y, Xiang K X, Zhang Y P, Xue J X. Honeycomb-like nitrogen and sulfur dual-doped hierarchical porous biomass-derived carbon for lithium-sulfur batteries[J]. ChemSusChem, 2017, 10(8): 1803-1812.

[8] Gan R Y, Yang N, Dong Q, Fu N, Wu R, Li C P, Liao Q, Li J, Wei Z D. Enveloping ultrathin Ti_3C_2 nanosheets on

carbon fibers: a high-density sulfur loaded lithium-sulfur battery cathode with remarkable cycling stability[J]. J. Mater. Chem. A, 2020, 8(15): 7253-7260.

[9] Chae C, Kim J, Kim J Y, Ji S, Lee S S, Kang Y, Choi Y, Suk J, Jeong S. Room-temperature, ambient-pressure chemical synthesis of amine-functionalized hierarchical carbon-sulfur composites for lithium-sulfur battery cathodes[J]. ACS Appl. Mater. Inter., 2018, 10(5): 4767-4775.

[10] ZhangY J, Liu X L, Wu L, Dong W D, Xia F J, Chen L D, Zhou N, Xia L X, Hu Z Y, Liu J, Mohamed H S H, Yu Li, Zhao Y, Chen Li H, Su B L. Flexible hierarchically PANI/MnO_2 porous network with fast channels and extraordinary chemical process for stable fastcharging lithium-sulfur battery[J]. J. Mater. Chem. A, 2020, 8: 2741-2751.

[11] Abualela S M, Lü X X, Hu Y, Abd-Alla, M D. NiO nanosheets grown on carbon cloth as mesoporous cathode for High-performance lithium-sulfur battery[J]. Mater. Lett., 2020, 268: 127622 .

[12] Yu F Q, Zhou H, Shen Q. Modification of cobalt-containing MOF-derived mesoporous carbon as an effective sulfur-loading host for rechargeable lithium-sulfur batteries [J]. J. Alloys Compd., 2019, 772: 843-851.

[13] Chen T, Cheng B R, Zhu G Y, Chen R P, Hu Y, Ma L B, Lü H L, Wang Y R, Liang J, Tie Z X, Jin Z, Liu J. Highly efficient retention of polysulfides in “sea urchin”-like carbon nanotube/nanopolyhedra superstructures as cathode material for ultralong-life lithium-sulfur batteries[J]. Nano Lett., 2016, 17(1): 437-444.

[14] Hu K, Wen J, Yan W Q, Zhu Y S, Zhang Y, Yu N F, Wu Y P. A three-dimensional interconnected nitrogen-doped graphene-like porous carbon-modified separator for high-performance Li-S batteries[J]. Sustain. Energy Fuels, 2020, 4(8): 4264-4272.

[15] Wu K(吴凯). Preparation and process optimization of cathode materials for lithium-sulfur batteries[J]. J. Electrochem.(电化学), 2020, 26(6): 825-833.

[16] Cui Z, He S A, Liu Q, Zou R J. Multifunctional $NiCo_2O_4$ nanosheet-assembled hollow nanoflowers as a highly efficient sulfur host for lithium-sulfur batteries[J]. Dalton Trans., 2020, 49(20): 6876-6883.

[17] Wang C G, Song H W, Yu C C, Ullah Z, Guan Z X, Chu R R, Zhang Y F, Zhao L Y, Li Q, Liu L W. Iron single atom catalyst anchored on nitrogen-rich MOF derived carbon nanocage to accelerate polysulfide redox conversion for lithium sulfur batteries[J]. J. Mater. Chem. A, 2020, 8(6): 3421-3430.

[18] Du Z Z, Chen X J, Hu W, Chuang C H, Xie S, Hu A J, Yan W S, Kong X H, Wu X J, Ji H X, Wan L J. Cobalt in nitrogen-doped graphene as single-atom catalyst for high-sulfur content lithium-sulfur batteries[J]. J. Am. Chem. Soc., 2019, 141(9): 3977-3985.

[19] Li Z, Yan J, Yuan L X, Yi Z Q, Wu C, Liu Y, Strasser P, Huang Y H. A Highly ordered meso@microporous carbon-supported sulfur@smaller sulfur core-shell structured cathode for Li-S batteries[J]. ACS Nano, 2014, 8(9): 9295-9303.

[20] Liu Y Z, Li G R, Chen Z W, Peng X S. CNT-threaded N-doped porous carbon film as binder-free electrode for high-capacity supercapacitor and Li-S battery[J]. J. Mater. Chem. A, 2017, 5(20): 9775-9784.

[21] Lei T Y, Chen W, Huang J W, Yan C Y, Sun H X, Wang C, Zhang W L, Li Y R, Xiong J. Multi-Functional layered WS_2 nanosheets for enhancing the performance of lithium-sulfur batteries[J]. Adv. Energy Mater., 2017, 7(4): 1601843.

[22] Xu W, Pang H M, Zhou H L, Jian Z X, Hu R M, Xing Y L, Zhang S C. Lychee-like TiO_2@TiN dual-function composite material for lithium-sulfur batteries[J]. RSC Adv., 2020, 10(5): 2670-2676.

[23] Feng X H, Wang Q, Li R R, Li H. $CoFe_2O_4$ coated carbon fiber paper fabricated via a spray pyrolysis method for trapping lithium polysulfide in Li-S batteries[J]. Appl. Surf. Sci., 2019, 478: 341-346.

[24] Shi J N, Kang Q, Mi Y, Xiao Q Q. Nitrogen-doped hollow porous carbon nanotubes for high-sulfur loading Li-S batteries[J]. Electrochim. Acta, 2019, 19: 31720-31727.

[25] Liu J T, Xiao S H, Zhang Z Y, Chen Y, Xiang Y, Liu X Q, Chen J S, Chen P. Naturally derived honeycomb-like N,S-codoped hierarchical porous carbon with MS_2 (M = Co, Ni) decoration for high-performance Li-S battery[J]. Nanoscale, 2020, 12(8): 5114-5124.

[26] Cai D, Liu B K, Zhu D H, Chen D, Lu M J, Cao J M, Wang Y H, Huang W H, Shao Y, Tu H R, Han W. Ultrafine Co_3Se_4 nanoparticles in nitrogen-doped 3D carbon matrix for high-stable and long-cycle-life lithium sulfur batteries[J]. Adv. Energy Mater., 2020, 10(19): 1904273.

[27] Huang M, Yang J Y, Xi B J, Mi K, Feng Z Y, Liu J, Feng J K, Qian Y T, Xiong S L. Enhancing kinetics of Li-S batteries by graphene-like N,S-codoped biochar fabricated in NaCl non-aqueous ionic liquid[J]. Sci. China Mater., 2018, 62(4): 455-464.

[28] Li N, Chen K H, Chen S Y, Wang F, Wang D D, Gan F Y, He X, Huang Y C. Manipulating the redox kinetics of Li-S chemistry by porous hollow cobalt - B, N codoped-graphitic carbon polyhedrons for high performance lithi-

um-sulfur batteries[J]. Carbon, 2019, 149: 564-571.

[29] Li J R, Zhou J, Wang T, Chen X, Zhang Y X, Wan Q, Zhu J. Covalent sulfur embedding in inherent N,P co-doped biological carbon for ultrastable and high rate lithium-sulfur batteries[J]. Nanoscale, 2020, 12(16): 8991-8996.

[30] Hu C J, Chang Y N, Chen R D, Yang J J, Xie T H, Chang Z, Zhang G X, Liu W, Sun X M. Polyvinylchloride-derived N, S co-doped carbon as an efficient sulfur host for high-performance Li-S batteries[J]. RSC Adv., 2018, 8(66): 37811-37816.

[31] Jiao S, Ding T Y, Zhai R, Wu Y P, Chen S, Wei W. Effective accommodation and conversion of polysulfides using organic-inorganic hybrid frameworks for long-life lithium-sulfur batteries[J]. Nanoscale, 2020, 12(25): 13377-13387.

[32] Gu W T, Sevilla M, Magasinski A, Fuertes A B, Yushin G. Sulfur-containing activated carbons with greatly reduced content of bottle neck pores for double-layer capacitors: a case study for pseudocapacitance detection[J]. Energy Environ. Sci., 2013, 6(8): 2465-2476.

[33] Du M Q, Meng Y S, Duan C Y, Wang C, Zhu F L, Zhang Y. Nitrogen-sulfur co-doped porous carbon prepared using ionic liquids as a dual heteroatom source and their application for Li-ion batteries[J]. J. Mater. Sci. - Mater. Electron., 2018, 29(21): 18179-18186.

[34] Zhang H, Zhao W Q, Zou M C, Wang Y S, Chen Y J, Xu L, Wu H S, Cao A Y. 3D, Mutually embedded MOF@carbon nanotube hybrid networks for high-performance lithium-sulfur batteries[J]. Adv. Energy Mater., 2018, 8(19): 1800013.

[35] Zeng L C, Pan F S, Li W H, Jiang Y, Zhong X W, Yu Y. Free-standing porous carbon nanofibers-sulfur composite for flexible Li-S battery cathode[J]. Nanoscale, 2014, 6(16): 9579-9607.

[36] Zhang Q F, Qiao Z S, Cao X R, Qu B H, Yuan J, Fan T E, Zheng H F, Cui J Q, Wu S Q, Xie Q S, Peng D L. Rational integration of spatial confinement and polysulfide conversion catalysts for high sulfur loading lithium-sulfur batteries[J]. Nanoscale Horiz., 2020, 5(4): 720-729.

[37] Jin J, Cai W L, Cai J S, Shao Y L, Song Y Z, Xia Z, Zhang Q, Sun J Y. MOF-derived hierarchical CoP nanoflakes anchored on vertically erected graphene scaffolds as self-supported and flexible hosts for lithium-sulfur batteries[J]. J. Mater. Chem. A, 2020, 8(6): 3027-3034.

[38] Meng Q H(孟全华), Deng W W(邓雯雯), Li C M(李长明). Facile synthesis of nitrogen-doped graphene-like active carbon materials for high performance lithium-sulfur battery[J]. J. Electrochem(电化学), 2020, 26(5): 740-749.

[39] Liu J P, Li Z, Jia B B, Zhu J C, Zhu W L, Li J P, Pan H, Zheng B W, Chen L Y, Pezzotti G, Zhu J L. A freestanding hierarchically structured cathode enables high sulfur loading and energy density of flexible Li-S batteries[J]. J. Mater. Chem. A, 2020, 8(13): 6303-6310.

[40] Li S Q, Mou T, Ren G F, Warzywoda J, Wang B, Fan Z Y. Confining sulfur species in cathodes of lithium-sulfur batteries: insight into nonpolar and polar matrix surfaces [J]. ACS Energy Lett., 2016, 1(2): 481-489.

[41] Lee J Y, Park G D, Choia J H, Kang Y C. Structural combination of polar hollow microspheres and hierarchical N-doped carbon nanotubes for high-performance Li-S batteries[J]. Nanoscale, 2020, 12(3): 2142-2153.

Nitrogen-Sulfur Co-Doped Porous Carbon Preparation and Its Application in Lithium-Sulfur Batteries

Gui-Xiang Zhao[1], Wail Hafiz Zaki Ahmed[1], Fu-Liang Zhu[1,2*]

(*1. School of Materials Science and Engineering, Lanzhou University of Technology, Lanzhou 730050, Gansu, China; 2. State Key Laboratory of Advanced Processing and Recycling of Nonferrous Metals, Lanzhou 730050, Gansu, China*)

Abstract: In recent years, lithium-sulfur (Li-S) batteries have been considered as a promising candidate for the next generation of energy storage system due to their ultrahigh theoretical capacity (1675 $mAh\cdot g^{-1}$) and energy density (2600 $Wh\cdot kg^{-1}$). However, the practical application of Li-S batteries is seriously limited by their insu lating nature of sulfur, the shuttle effect of polysulfides (LiPSs), and volume expansion during charging and discharging. To overcome those disadvantages, one of the commonly methods is to infiltrate sulfur into porous conductive carbon framework, such as porous carbon, hollow carbon spheres, graphene, carbon nanotubes and some composites of the above structures to achieve the purpose of physically limiting the shuttle effect of polysulfides, thereby improving the performance of Li-S batteries. However, due to the nonpolarity of traditional carbon materials, the interaction with polar polysulfides is very weak, which cannot effectively inhibit the shuttle effect of polysulfides. Previous studies have shown that introducing heteroatom (N, S, P, B, etc.) doping into carbon matrix is a feasible method to adjust the nonpolarity of carbon materials. It is reported that the introduction of N atoms is conducive to improving the electrochemical activity. The Li-N bond formed by the interaction between N and Li^+ can anchor polysulfides, effectively inhibit the dissolution of polysulfides and improve the utilization rate of sulfur. The introduction of nitrogen and sulfur heteroatoms can increase polar sites and active centers, thus, enhancing the adsorption capacity of carbon materials for polysulfides and capturing polysulfides. Therefore, ionic liquids are selected as nitrogen and sulfur sources to improve the polarity of carbon materials. In this paper, nitrogen and sulfur co-doped porous carbon (NSPC) was synthesized by using glucose as carbon source, KCl and $ZnCl_2$ as templates, KOH as activator and ionic liquid as heteroatom source. XPS and adsorption experiments show that nitrogen and sulfur heteroatoms had been successfully introduced into NSPC, which improved the adsorption capacity of carbon materials for polysulfides, effectively alleviated the shuttle effect of polysulfides. The higher specific surface area (1290.67 $m^2\cdot g^{-1}$) could help to improve the sulfur loading. After loading 70.1wt.% sulfur into NSPC (S@NSPC) and tested as a cathode material of Li-S battery, the initial discharge capacity was 1229.2 $mAh\cdot g^{-1}$ at 167.5 $mA\cdot g^{-1}$, higher than the 861.6 $mAh\cdot g^{-1}$ of S@PC, and the capacity remained at 328.1 $mAh\cdot g^{-1}$ after 500 cycles. When the current density returned to 167.5 $mA\cdot g^{-1}$, the reversible capacity almost went back to its initial value, which was 80% of its initial value. The good performance was mainly ascribed to both the porous structure and N, S co-dopants, which provided physical blocks and chemical affinity, respectively, for the efficient immobilization of intermediate lithium polysulfides. The results would provide an effective example in the surface chemistry and sulfur host materials design for high performance Li-S batteries.

Key words: lithium-sulfur batteries; porous carbon; heteroatom doping